Scattering properties of needlelike and platelike ice spheroids with moderate size parameters

Nadia T. Zakharova and Michael I. Mishchenko

We use the current advanced version of the T-matrix method to compute the optical cross sections, the asymmetry parameter of the phase function, and the scattering matrix elements of ice spheroids with aspect ratios up to 20 and surface-equivalent-sphere size parameters up to 12. We demonstrate that platelike and needlelike particles with moderate size parameters possess unique scattering properties: their asymmetry parameters and phase functions are similar to those of surface-equivalent spheres, whereas all other elements of the scattering matrix are typical of particles much smaller than the wavelength (Rayleigh scatterers). This result may have important implications for optical particle sizing and remote sensing of the terrestrial and planetary atmospheres.

OCIS codes: 010.1110, 010.1290, 010.1310, 010.2940, 290.1090, 290.1310.

1. Introduction

Several recent publications have taken advantage of the improved version of the T-matrix method[1] and presented an extensive survey of light-scattering properties of polydisperse, randomly oriented spheroids with moderate aspect ratios (see, e.g., Refs. 2 and 3 and references therein). However, the results from Refs. 4–6 indicate that spheroids with extreme aspect ratios may have scattering properties dramatically different from those of moderately aspherical particles. Therefore, in this paper we calculate the optical cross sections, the asymmetry parameter, and the scattering matrix for randomly oriented ice spheroids with aspect ratios up to 20 and equivalent-sphere size parameters up to 12 and compare them with analogous results for surface-equivalent spheres and spheroids with an aspect ratio of 2. Because needlelike and platelike particles can be abundant in various natural and artificial environments, we conclude the paper by a discussion of potential practical implications of our results.

N. T. Zakharova (crntz@giss.nasa.gov) is with Science Systems and Applications, Incorporated, 2880 Broadway, New York, New York 10025. M. I. Mishchenko is with the NASA Goddard Institute for Space Studies, 2880 Broadway, New York, New York 10025.

Received 9 March 2000; revised manuscript received 3 July 2000.

0003-6935/00/275052-06$15.00/0

2. Computations

We performed calculations for five particle shapes: spheres, prolate spheroids with semiaxis ratios $a/b = 0.5$ and 0.05, and oblate spheroids with $a/b = 2$ and 20, where b is the rotation (vertical) semiaxis and a is the horizontal semiaxis of a spheroid. The size of a spheroid was specified in terms of the radius of the surface-equivalent sphere r_s (or, equivalently, the radius of the sphere having the same projected area[7]). To suppress the interference structure in light-scattering patterns (Refs. 2, 3, and 8), the computation results for spheres and spheroids with $a/b = 0.5$ and 2 were averaged over a narrow gamma distribution of equivalent-sphere radii given by[8]

$$n(r_s) = \frac{1}{r_{s,\mathrm{eff}}\nu_{\mathrm{eff}}\Gamma\left(\frac{1-2\nu_{\mathrm{eff}}}{\nu_{\mathrm{eff}}}\right)}\left(\frac{r_s}{r_{s,\mathrm{eff}}\nu_{\mathrm{eff}}}\right)^{(1-3\nu_{\mathrm{eff}})/\nu_{\mathrm{eff}}} \times \exp\left(-\frac{r_s}{r_{s,\mathrm{eff}}\nu_{\mathrm{eff}}}\right), \quad (1)$$

with an effective variance of $\nu_{\mathrm{eff}} = 0.05$. Table 1 lists the surface-equivalent-sphere size parameters $x_s = 2\pi r_s/\lambda$ (for monodisperse spheroids with $a/b = 0.05$ and 20) and effective surface-equivalent-sphere size parameters $x_{s,\mathrm{eff}} = 2\pi r_{s,\mathrm{eff}}/\lambda$ (for spheres and polydisperse spheroids with $a/b = 0.5$ and 2) used in our computations, where λ is the wavelength of the incident light. The maximal values of x_s for spheroids with $a/b = 0.05$ and 20 were limited by the growing

Table 1. Equal-Surface-Sphere Size Parameters x_s (or $x_{s,\mathrm{eff}}$), Equal-Volume-Sphere Size Parameters x_v (or $x_{v,\mathrm{eff}}$), and Size Parameters along the Horizontal, x_a (or $x_{a,\mathrm{eff}}$), and Vertical, x_b (or $x_{b,\mathrm{eff}}$), Spheroid Axes Used in the *T*-Matrix Computations

x_s	x_v	x_a	x_b
$a/b = 0.05$			
0.1	0.0684	0.0252	0.5043
1	0.6845	0.2522	5.0432
2	1.3690	0.5043	10.087
3.5	2.3957	0.8826	17.651
$a/b = 20$			
0.1	0.0519	0.1408	0.0070
1	0.5186	1.4077	0.0704
2	1.0372	2.8155	0.1408
3.5	1.8151	4.9271	0.2464
6	3.1117	8.4464	0.4223
9	4.6675	12.670	0.6335
12	6.2233	16.893	0.8446
$x_{s,\mathrm{eff}}$	$x_{v,\mathrm{eff}}$	$x_{a,\mathrm{eff}}$	$x_{b,\mathrm{eff}}$
$a/b = 0.5$			
0.1	0.0964	0.0765	0.1530
1	0.9637	0.7649	1.5298
2	1.9274	1.5298	3.0596
3.5	3.3730	2.6771	5.3543
6	5.7823	4.5894	9.1788
9	8.6734	6.8841	13.768
12	11.565	9.1788	18.358
$a/b = 2$			
0.1	0.0955	0.1204	0.0602
1	0.9554	1.2038	0.6019
2	1.9109	2.4076	1.2038
3.5	3.3441	4.2132	2.1066
6	5.7327	7.2227	3.6114
9	8.5990	10.834	5.4170
12	11.465	14.445	7.2227

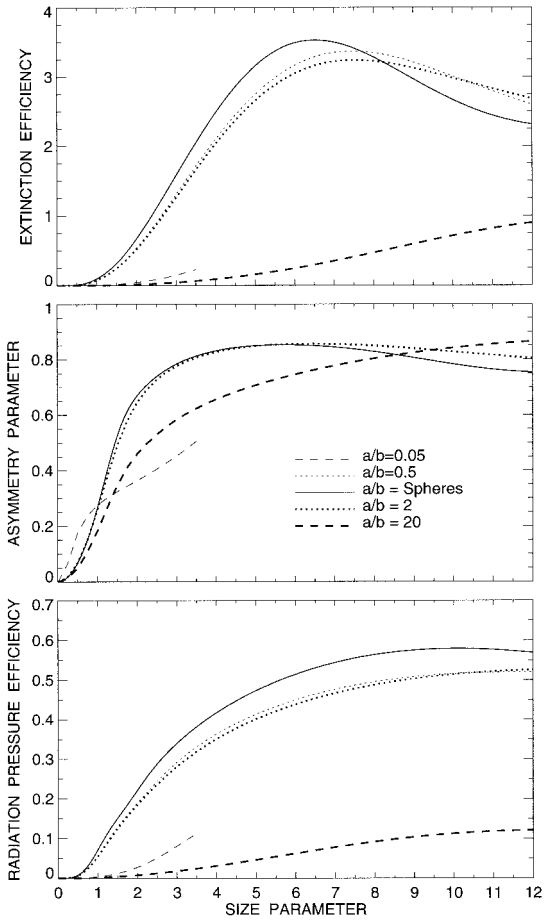

Fig. 1. Extinction efficiency factor, asymmetry parameter, and radiation pressure efficiency factor versus surface-equivalent-sphere size parameter for spheres and randomly oriented spheroids with various semiaxis ratios. Note that the asymmetry parameter curves for spheroids with $a/b = 0.5$ and 2 almost coincide.

numerical instability of *T*-matrix computations caused by a finite number of decimals in the computer representation of real variables.[1] For comparison, Table 1 also lists the corresponding values of the equal-volume-sphere size parameters $x_v = 2\pi r_v/\lambda$ and $x_{v,\mathrm{eff}} = 2\pi r_{v,\mathrm{eff}}/\lambda$, as well as the respective size parameters along the horizontal and the vertical spheroid axes $x_a = 2\pi a/\lambda$, $x_{a,\mathrm{eff}} = 2\pi a_{\mathrm{eff}}/\lambda$, $x_b = 2\pi b/\lambda$, and $x_{b,\mathrm{eff}} = 2\pi b_{\mathrm{eff}}/\lambda$. The refractive index was fixed at 1.311, which is a typical value for water ice at visible wavelengths.[9]

Figure 1 shows the efficiency factor for extinction $Q_{\mathrm{ext}} = \langle C_{\mathrm{ext}}\rangle/\langle G\rangle$, the asymmetry parameter of the phase function (or average cosine of the scattering angle) $\langle\cos\Theta\rangle$, and the efficiency factor for radiation pressure $Q_{\mathrm{pr}} = Q_{\mathrm{ext}}(1 - \langle\cos\Theta\rangle)$, where $\langle C_{\mathrm{ext}}\rangle$ is the ensemble-averaged scattering cross section per particle and $\langle G\rangle$ is the average area of the particle geometric projection. Because the imaginary part of the refractive index is zero, the efficiency factor for scattering is equal to Q_{ext} and the single-scattering albedo is identically equal to unity.

Figures 2 and 3 show the phase function $a_1(\Theta)$ and the normalized elements of the Stokes scattering matrix[10]

$$\begin{bmatrix} a_1(\Theta) & b_1(\Theta) & 0 & 0 \\ b_1(\Theta) & a_2(\Theta) & 0 & 0 \\ 0 & 0 & a_3(\Theta) & b_2(\Theta) \\ 0 & 0 & -b_2(\Theta) & a_4(\Theta) \end{bmatrix}, \tag{2}$$

where Θ is the scattering angle. The phase function satisfies the normalization condition

$$1/2\int_0^{\pi} \mathrm{d}\Theta a_1(\Theta)\sin\Theta = 1. \tag{3}$$

Note that for spheres $a_2(\Theta)/a_1(\Theta) \equiv 1$ and $a_3(\Theta) \equiv a_4(\Theta)$.

3. Discussion

Figures 2 and 3 show that needlelike and platelike particles with moderate equivalent-sphere size parameters possess unique scattering properties. Indeed, their phase functions are similar to those of

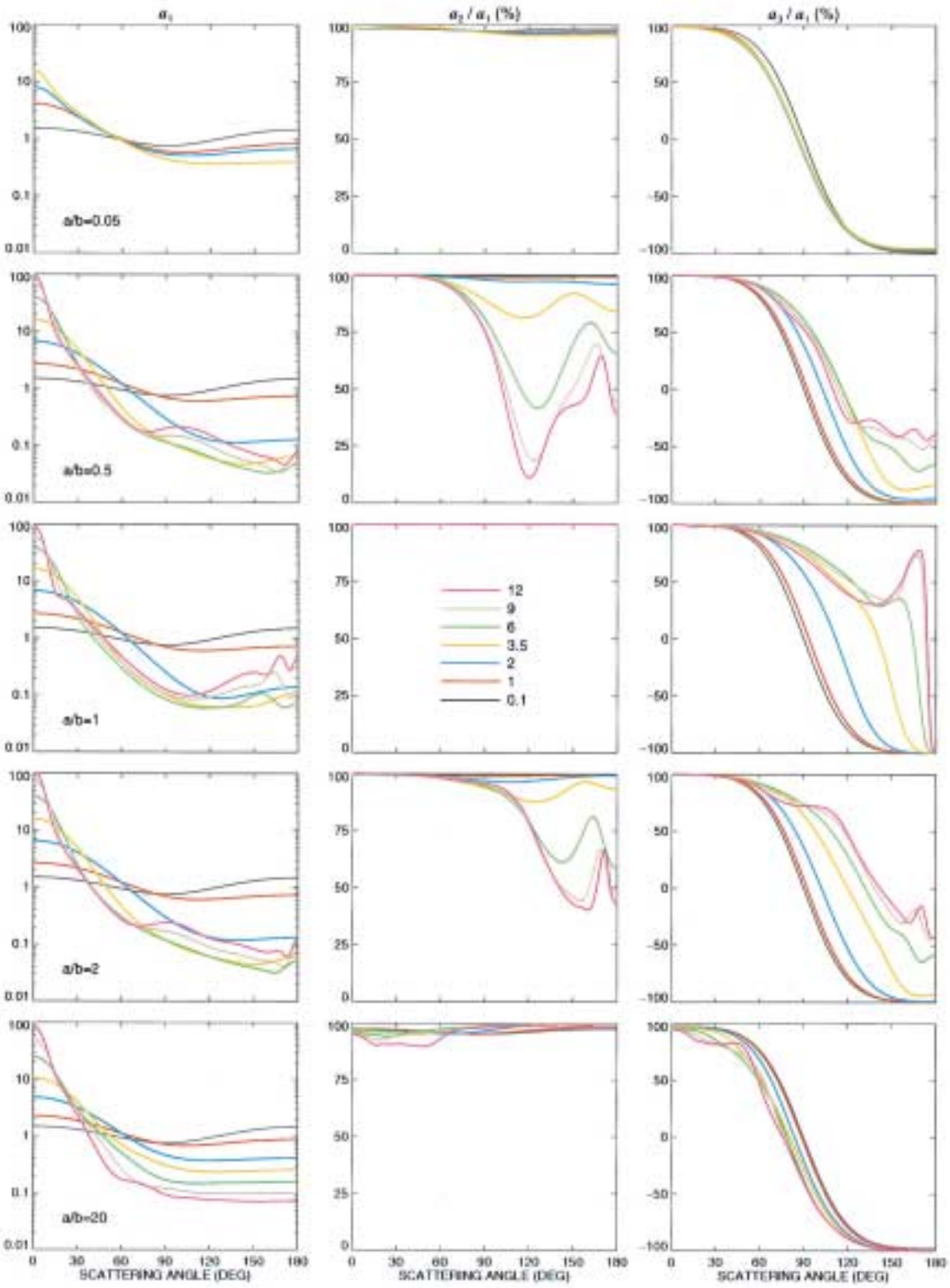

Fig. 2. Phase function and normalized elements of the scattering matrix for spheres and surface-equivalent, randomly oriented spheroids with size parameters ranging from 0.1 to 12 (see color legend) and semiaxis ratios $a/b = 0.05$ (first row), 0.5 (second row), 1 (third row), 2 (fourth row), and 20 (fifth row).

equivalent spheres and spheroids with moderate aspect ratios and have a pronounced forward-scattering lobe, whereas all other elements of the scattering matrix closely resemble those of particles much smaller than the wavelength (Rayleigh scatterers). In particular, all linear polarization curves $(-b_1/a_1)$

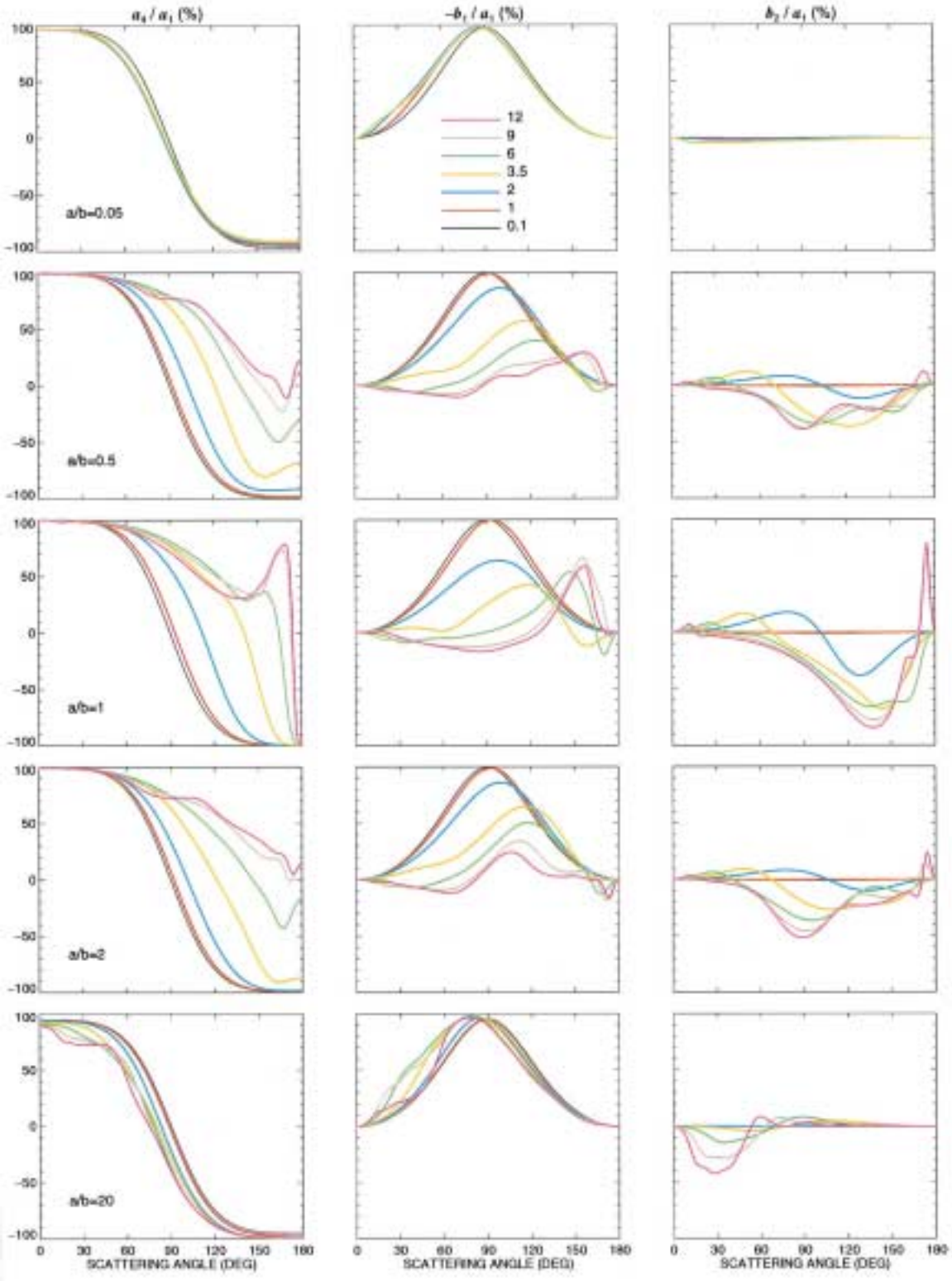

Fig. 3. Normalized elements of the scattering matrix for spheres and surface-equivalent, randomly oriented spheroids with size parameters ranging from 0.1 to 12 (see color legend) and semiaxis ratios $a/b = 0.05$ (first row), 0.5 (second row), 1 (third row), 2 (fourth row), and 20 (fifth row).

for the spheroids with $a/b = 0.05$ and 20 have a characteristic bell-like shape with a maximum reaching nearly 100% at scattering angles close to 90°. The ratio $a_2(\Theta)/a_1(\Theta)$ is close to unity, and the elements $a_3(\Theta)$ and $a_4(\Theta)$ are nearly the same. The fact that $a_2(\pi) \approx a_1(\pi)$ and $a_4(\pi) \approx -a_1(\pi)$ makes the

linear, $\delta_L = [a_1(\pi) - a_2(\pi)]/[a_1(\pi) + a_2(\pi)]$, and the circular, $\delta_C = [a_1(\pi) + a_4(\pi)]/[a_1(\pi) - a_4(\pi)]$, depolarization ratios[11] close to zero. In contrast, wavelength-sized spheroids with $a/b = 0.5$ and 2 cause significant backscattering depolarization. This demonstrates once again that the magnitude of the depolarization ratios is not a universal indicator of the degree of particle asphericity (see Refs. 11 and 12). The extinction and radiation pressure efficiency factors for the highly aspherical spheroids are significantly smaller than those for spheres and moderately aspherical spheroids having the same area of geometric projection, whereas the values of the asymmetry parameter are similar. This is another indication that the scattering properties of platelike and needlelike spheroids with moderate size parameters resemble those of Rayleigh particles as well as surface-equivalent spheres.

The linear polarization curves for spheres show that the regime of Rayleigh scattering breaks at size parameters close to 1. According to Table 1, the size parameter along the shorter semiaxis of the spheroids with $a/b = 0.05$ and 20 is smaller than unity even for the largest x_s values used. Therefore, our computations might indicate that the asymmetry parameter and the phase function are determined mostly by the value of the size parameter of the sphere having the same projected area, whereas all other elements of the scattering matrix and the optical cross sections are more sensitive to the value of the size parameter along the smallest particle dimension. It is interesting to note in this regard that West[13] found similar features in light scattering by low-density aggregates of spheres with outer diameters comparable to the wavelength and monomer sizes much smaller than the wavelength. He concluded that the forward-scattering lobe of the phase function was representative of the mean projected area of the cluster, whereas the angular dependence of the linear polarization depended on the monomer diameter.

Our results may have important ramifications for optical particle sizing, remote sensing of the Earth's and planetary atmospheres, and astrophysics. For example, the fact that the size-parameter dependence of the extinction efficiency factor for platelike and needlelike particles is significantly different from that for spherical and moderately aspherical particles (upper panel of Fig. 1) could influence the results of particle sizing by use of spectral measurements of extinction. The much lower values of the efficiency for radiation pressure for highly aspherical particles (lower panel of Fig. 1) could affect the magnitude of the radiation force exerted on interstellar and interplanetary grains by starlight. The weak depolarization capability of highly aspherical particles should be taken into account during analysis of lidar depolarization measurements.[12,14] Another example is the well-known observation that the degree of linear polarization of visible sunlight scattered by noctilucent particles at scattering angles close to 90° often reaches nearly 100%.[15,16] This observation was traditionally interpreted in terms of an average cloud particle size less than 0.1 μm, but this conclusion might need to be revisited in view of our results (see Ref. 4). Haze particles in the stratosphere of Titan are also known to possess unusual scattering properties. They produce strong linear polarization at side-scattering angles characteristic of spherical particles with radii smaller than 0.1 μm, whereas the angular distribution of scattered intensity at forward-scattering angles is typical of significantly larger particles.[17] A similar problem exists for Jupiter's stratospheric haze.[18,19] West and Smith[17] concluded that spheroids with aspect ratios less than 4 could not possess such scattering properties. Our calculations for significantly larger aspect ratios show that wavelength-sized spheroids can possess these properties and can be used as candidate particles in analyses of the observations of Titan and Jupiter.

This research was sponsored by the NASA Radiation Science Program managed by Robert Curran.

References

1. M. I. Mishchenko and L. D. Travis, "Capabilities and limitations of a current FORTRAN implementation of the *T*-matrix method for randomly oriented, rotationally symmetric scatterers," J. Quant. Spectrosc. Radiat. Transfer **60,** 309–324 (1998).
2. M. I. Mishchenko, L. D. Travis, and D. W. Mackowski, "*T*-matrix computations of light scattering by nonspherical particles: a review," J. Quant. Spectrosc. Radiat. Transfer **55,** 535–575 (1996).
3. M. I. Mishchenko, L. D. Travis, and A. Macke, "*T*-matrix method and its applications," in *Light Scattering by Nonspherical Particles: Theory, Measurements, and Applications*, M. I. Mishchenko, J. W. Hovenier, and L. D. Travis, eds. (Academic, San Diego, Calif., 2000), pp. 147–172.
4. M. I. Mishchenko, "Light scattering by nonspherical ice grains: an application to noctilucent cloud particles," Earth Moon Planets **57,** 203–211 (1992).
5. F. Kuik, J. F. de Haan, and J. W. Hovenier, "Single scattering of light by circular cylinders," Appl. Opt. **33,** 4906–4918 (1994).
6. F. M. Schulz, K. Stamnes, and J. J. Stamnes, "Shape dependence of the optical properties in size-shape distributions of randomly oriented prolate spheroids, including highly elongated shapes," J. Geophys. Res. **104,** 9413–9421 (1999).
7. V. Vouk, "Projected area of convex bodies," Nature (London) **162,** 330–331 (1948).
8. J. E. Hansen and L. D. Travis, "Light scattering in planetary atmospheres," Space Sci. Rev. **16,** 527–610 (1974).
9. S. G. Warren, "Optical constants of ice from the ultraviolet to the microwave," Appl. Opt. **23,** 1206–1225 (1984).
10. M. I. Mishchenko, J. W. Hovenier, and L. D. Travis, "Concepts, terms, notation," in *Light Scattering by Nonspherical Particles: Theory, Measurements, and Applications*, M. I. Mishchenko, J. W. Hovenier, and L. D. Travis, eds. (Academic, San Diego, Calif., 2000), pp. 3–27.
11. M. I. Mishchenko and J. W. Hovenier, "Depolarization of light backscattered by randomly oriented nonspherical particles," Opt. Lett. **20,** 1356–1358 (1995).
12. M. I. Mishchenko and K. Sassen, "Depolarization of lidar returns by small ice crystals: an application to contrails," Geophys. Res. Lett. **25,** 309–312 (1998).
13. R. A. West, "Optical properties of aggregate particles whose

outer diameter is comparable to the wavelength," Appl. Opt. **30,** 5316–5324 (1991).
14. K. Sassen, "Lidar backscatter depolarization technique for cloud and aerosol research," in *Light Scattering by Nonspherical Particles: Theory, Measurements, and Applications*, M. I. Mishchenko, J. W. Hovenier, and L. D. Travis, eds. (Academic, San Diego, Calif., 2000), pp. 393–416.
15. W. F. Tozer and D. E. Beeson, "Optical model of noctilucent clouds based on polarimetric measurements from two sounding rocket campaigns," J. Geophys. Res. **79,** 5607–5612 (1974).
16. G. Witt, J. E. Dye, and N. Wilhelm, "Rocket-borne measurements of scattered sunlight in the mesosphere," J. Atmos. Terrestrial Phys. **38,** 223–238 (1976).
17. R. A. West and P. H. Smith, "Evidence for aggregate particles in the atmospheres of Titan and Jupiter," Icarus **90,** 330–333 (1991).
18. M. G. Tomasko, R. A. West, and N. D. Castillo, "Photometry and polarimetry of Jupiter at large phase angles. I. Analysis of imaging data of a prominent belt and a zone from Pioneer 10," Icarus **33,** 558–592 (1978).
19. P. Smith, "The vertical structure of the Jovian atmosphere," Icarus **65,** 264–279 (1986).